

## Dynamics of a drop at a fluid interface under shear

K. A. Smith\* and J. M. Ottino

*Department of Chemical Engineering, Northwestern University, Evanston, Illinois 60208, USA*

M. Olvera de la Cruz

*Department of Materials Science and Engineering, Northwestern University, Evanston, Illinois 60208, USA*

(Received 22 October 2003; published 15 April 2004)

We analyze the dynamics of a two-dimensional drop lying on a fluid interface, sometimes called a liquid lens, subjected to simple shear flow. The three fluids, the drop and the two external fluids, meet at a triple point (or a triple line in three dimensions). A requirement for steady drop shapes is that the triple points are stationary. This leads to a flow topology different than that of a freely suspended drop. Results are substantiated with numerical results using a level set method for interface evolution and treatment of triple points. Possible implications for new drop instabilities are also discussed.

DOI: 10.1103/PhysRevE.69.046302

PACS number(s): 47.85.Dh

### I. INTRODUCTION

The effect of flow in the mixing of immiscible fluids is a fundamental problem in the processing of incompatible materials [1,2]. In many cases extra components are added to the incompatible materials to increase their miscibility. In polymer blends, for example, minority components are added to decrease the interfacial energy and/or to improve the mechanical properties of the final material [3]. The minority component segregates at the interface of the majority components, where it often forms its own phase [4–6]. When flow is imposed to this multiphase fluid a series of morphological changes are expected. The segregation processes in incompatible binary fluids in the absence of shear [7–10] as well as the effect of shear flow on the decomposition [11–15] have been extensively studied. Flow in ternary fluids is more complicated since it may involve the deformation of a fluid drop at a fluid interface.

In a binary incompatible fluid the minority component forms drops. The response of a drop suspended in an external fluid to extensional and shear flows has been a topic of study since the pioneering work of Taylor [16] as reviewed in Refs. [17,18]. This scenario, which we refer to as a simple drop, has widespread relevance in many problems besides fluid mixing. In ternary fluids complicated morphologies occur when the range of interfacial tension is such that the three fluids meet at a stable triple point in two dimensions, or at a triple line in three dimensions. In this case no fluid wets the interface between the other two fluids. Thus a drop of a given fluid can remain confined to the interface between two external fluids. We call this an interfacial drop. The dynamics of interfacial drops is not only relevant to flow in multiphase bulk systems [19], but also in microchannels [20], to liquid lenses, surfactant monolayers, oil spills, and even to high-energy physics [21]. Significantly, the presence of the exter-

nal interface and the triple points affects both the steady and unsteady behaviors of the drop. This scenario appears to have been little studied to date, either analytically, experimentally, or numerically. In this paper we analyze interfacial drop flow by using kinematical arguments, and demonstrate our conclusions numerically. In the last section we discuss possible implications of our analysis on instabilities of interfacial drops under shear flow.

### II. SYSTEM DESCRIPTION

We consider the two-dimensional system illustrated in Fig. 1. The region of space occupied by phase  $i$  is labeled  $\Omega_i$ . The external fluids are  $\Omega_1$  and  $\Omega_2$  while the drop is  $\Omega_3$ . The boundary of  $\Omega_i$  is labeled  $\Gamma_i$  and the common interface between  $\Omega_i$  and  $\Omega_j$  is  $\Gamma_{ij}$  (i.e.,  $\Gamma_{ij} = \Gamma_i \cap \Gamma_j$ ). The triple points at the left and right tips of the drop are labeled  $L$  and  $R$ , respectively. The external flow, far from the drop, is simple shear,  $\mathbf{u}(\mathbf{x}) = (\dot{\gamma}y, 0)$ . The viscosity of  $\Omega_i$  is  $\mu_i$  and the interfacial tension on  $\Gamma_{ij}$  is  $\sigma_{ij}$ . Since the system is two dimensional,

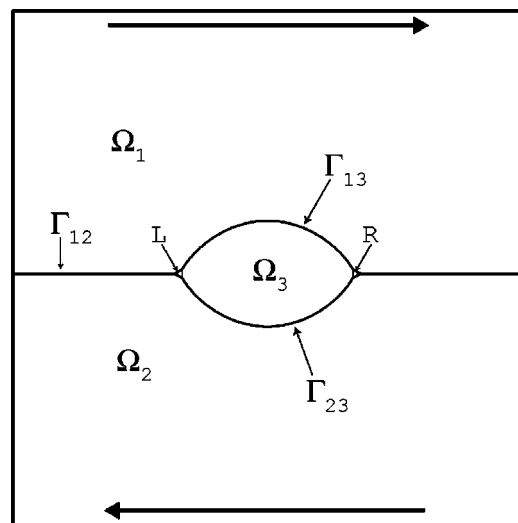


FIG. 1. Interfacial drop in shear flow.

\*Present address: LPMCN, Université Claude Bernard, 69622 Villeurbanne, France.

Electronic address: ksmith@lpmcn.univ-lyon1.fr

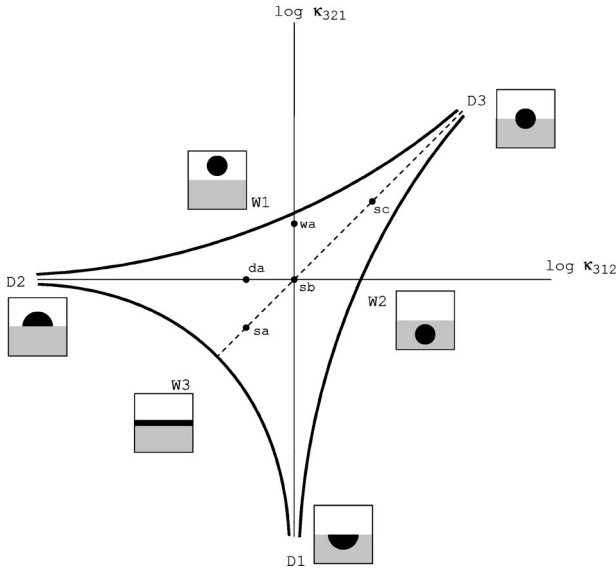


FIG. 2. Schematic diagram of the dependence of drop configuration on interfacial tensions. The drop is stable at the interface in the region between the three curves. The system has states  $W1$ ,  $W2$ , and  $W3$  outside this region, and states  $D1$ ,  $D2$ , and  $D3$  in the limit that one interfacial tension  $\rightarrow 0$  with the other two being equal. Asymmetric conformations occur at  $da$  and  $wa$ . Symmetric conformations occur at  $sa$ ,  $sb$ , and  $sc$ .

line tension at a triple line can be omitted from consideration. A characteristic drop length  $a$  is defined as the radius of a circular drop with the same area as  $\Omega_3$ . For all flows examined, here length scales are assumed to be sufficiently small that the system is dominated by viscous shear stresses and interfacial tension, thus we can neglect inertia ( $Re = \rho U a / \mu \rightarrow 0$ ) and gravity ( $Bo = \Delta \rho g a^2 / \sigma \rightarrow 0$ ). Viscosity ratios are expressed as  $\lambda_{ij} = \mu_i / \mu_j$  and interfacial tension ratios as  $\kappa_{ijk} = \sigma_{ij} / \sigma_{jk}$ . Then an interfacial drop can be described by five dimensionless parameters:  $\lambda_{21}$ ,  $\lambda_{31}$ ,  $\kappa_{321}$ ,  $\kappa_{312}$ , and a capillary number  $Ca = \mu_1 a \dot{\gamma} / \sigma_{13}$ . In this work we consider only cases where  $\lambda_{21} = \lambda_{31} = 1$ . When there is no external flow the equilibrium conformation is that which minimizes the total interfacial energy and is determined entirely by  $\kappa_{312}$  and  $\kappa_{321}$ . Equilibrium contact angles at  $L$  and  $R$  are given by the Neumann triangle relation

$$\sin(\pi - \theta_3) / \sigma_{12} = \sin(\pi - \theta_2) / \sigma_{13} = \sin(\pi - \theta_1) / \sigma_{23} \quad (1)$$

or equivalently

$$\sin(\pi - \theta_3) = \sin(\pi - \theta_2) / \kappa_{312} = \sin(\pi - \theta_1) / \kappa_{321}, \quad (2)$$

where  $\theta_i$  is the contact angle in  $\Omega_i$ . A given fluid  $\Omega_i$  wets  $\Gamma_{jk}$  when  $\sigma_{jk} > \sigma_{ij} + \sigma_{ik}$ . We refer to this wetting case as “ $Wi$ .” At the other extreme, where  $\sigma_{jk} \ll \sigma_{ij} + \sigma_{ik}$  the boundary  $\Gamma_i$  becomes flat at the triple point ( $\theta_i = \pi$ ). We refer to this case, where the interfacial tensions on  $\Gamma_i$  dominate the equilibrium conformation, as “ $Di$ .” A qualitative phase diagram illustrating all of these configurations is shown in Fig. 2. Each of the wetting cases  $W1$ ,  $W2$ , and  $W3$  occurs over a region of phase space bounded by an open curve. The region between the three curves represents the values of  $\kappa_{312}$  and  $\kappa_{321}$  for which

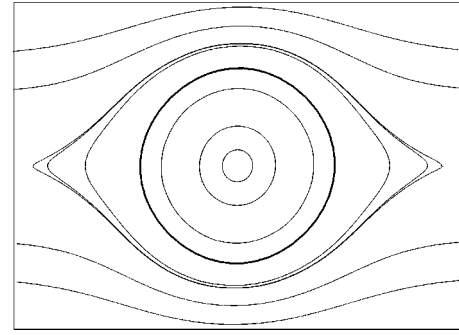


FIG. 3. Computed streamlines in the small deformation limit for a simple drop in shear flow. The drop interface is the largest circular streamline.

a stable triple point, and thus a stable interfacial drop, exists. The “dominant” cases  $D1$ ,  $D2$ , and  $D3$  are the equilibria in the limit where one of the interfacial tensions goes to zero and the other two are equal. This system has two degrees of freedom. By contrast, a solid sphere at a fluid interface has only one degree of freedom, the height of the sphere center of mass relative to the interface (curvature of the interface due to gravity is not considered here). The position of the drop center of mass can be varied in two distinct ways. Starting from the origin in Fig. 2 the drop center can be shifted upwards by increasing  $\sigma_{23}$  (moving up along the vertical axis in the phase diagram) or by decreasing  $\sigma_{13}$  (moving to the left along the horizontal axis). In the former case  $\theta_1 \rightarrow 0$  and the drop becomes circular as the  $W1$  curve is approached. In the latter case  $\theta_1 \rightarrow \pi/2$  and the drop becomes a semicircle in the  $D2$  limit.

### III. KINEMATICAL ARGUMENTS

The presence of the external interface  $\Gamma_{12}$  and the triple points  $L$  and  $R$  imposes a constraint on allowable steady state flows, namely, that the drop cannot rotate. The kinematical constraint in a steady state flow is that the velocity on any interface has no normal component. Consequently  $L$  and  $R$  must be stationary. For a simple drop, pure extensional flow produces recirculation inside the drop with four stationary points on the drop surface (see, for instance, Ref. [22]). Such a flow is compatible with an interfacial drop if two of the stationary points coincide with the triple points. In simple shear, however, the vorticity in the external flow causes a simple drop to rotate (see Fig. 3). Fluid elements on the drop surface lie on a closed streamline and return to their original positions in a finite amount of time. Closed streamlines also exist in the external fluid close to the drop or the (horizontal) centerline. Points farther away lie on open streamlines, which eventually move away from the drop in both forward and backward time. This flow field, a region of closed streamlines surrounded by open streamlines above and below, is topologically equivalent to a field containing two hyperbolic points with smoothly joined stable and unstable manifolds. The region of closed streamlines maps to the space bounded by the common manifolds. In fact for a peri-

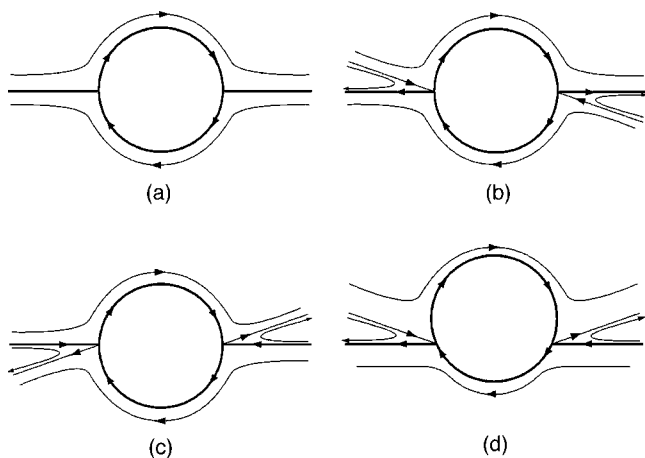


FIG. 4. Possible classes of flow in the vicinity of an interfacial drop. Interfaces (circular for the drop and horizontal between the bulk fluids) are only for illustration and do not represent actual interfacial shapes.

odic series of drops (such as when periodic boundary conditions are imposed numerically) hyperbolic points exist at the box borders and the flow is equivalent to the phase plane of a pendulum (see for example Ref. [23]). Since no stationary points exist on the drop surface this flow is not compatible with a steady interfacial drop. Instead a new type of flow occurs which must satisfy the following conditions.

(i) The boundary condition on the velocity is simple shear flow far above and below the drop.

(ii)  $L$  and  $R$  are stationary points of the flow (else a steady interface cannot exist).

(iii) There are no other stationary points on  $\Gamma_3$ . Points on  $\Gamma_{13}$  flow towards  $R$  and points on  $\Gamma_{23}$  flow towards  $L$  (since the system is highly viscous).

Four kinematically possible classes of flow exist which can be distinguished by the velocity on  $\Gamma_{12}$ . We refer to these as class  $A$ ,  $B$ ,  $C$ , and  $D$  flows as shown in Fig. 4. In class  $A$  flow  $\mathbf{u}=0$  on  $\Gamma_{12}$ , all points in  $\Omega_1$  move steadily to the right and all points in  $\Omega_2$  move to the left.  $L$  has one stable manifold ( $\Gamma_{23}$ ), one unstable manifold ( $\Gamma_{13}$ ), and one line of neutral stability ( $\Gamma_{12}$ ) (with a symmetrical situation at  $R$ ). If the flow on  $\Gamma_{12}$  is away from the drop (class  $B$ ) then  $\Gamma_{12}$  contains *unstable* manifolds of both  $L$  and  $R$ . To satisfy continuity there must be a stable manifold of  $L$  in  $\Omega_1$  and a stable manifold of  $R$  in  $\Omega_2$ .  $L$  and  $R$  are hyperbolic points and there is a recirculating region near each where elements flow towards the triple point initially and then away from it. For class  $C$  the flow on  $\Gamma_{12}$  is directed towards the drop so the *stable* manifolds of  $L$  and  $R$  lie on  $\Gamma_{12}$ . The unstable manifold of  $L$  lies in  $\Omega_2$  and that of  $R$  lies in  $\Omega_1$ . Class  $A$ ,  $B$ , and  $C$  flows all have a symmetry of rotation about the center line. In class  $D$  flow, which is not symmetric, all points on  $\Gamma_{12}$  flow in the same direction. The drop moves relative to  $\Gamma_{12}$  and both  $L$  and  $R$  have manifolds in the same external fluid ( $\Omega_1$  if the drop moves to the right and  $\Omega_2$  if it moves to the left). This is similar to the picture of a drop rolling over a solid surface proposed in Ref. [24].

#### IV. GOVERNING EQUATIONS AND NUMERICAL METHOD

We consider a system of three immiscible fluids where the viscosities and densities of all fluids are taken to be equal. The fluids are incompressible and are governed by the Navier-Stokes equations.

$$\frac{\partial \mathbf{u}}{\partial t} = -\nabla p - \mathbf{u} \cdot \nabla \mathbf{u} + (1/\text{Re})\nabla^2 \mathbf{u} - \mathbf{F}, \quad (3)$$

$$\nabla \cdot \mathbf{u} = 0, \quad (4)$$

where  $\mathbf{F}$  is the interfacial tension force. We set  $\text{Re}=0.1$  which is sufficiently small that interfacial effects are negligible. The method used for representing the interface is a level set algorithm, as developed in Refs. [25,26], with a continuum treatment of interfacial tension [27]. This method has been extended to track interfaces in ternary fluids [19], and compute the motion of triple lines [28]. There are several viable techniques for representing fluid interfaces such as boundary integral and volume-of-fluid methods. Distinct advantages of the level set method include a natural handling of topological changes in the interface, easy extension to any number of spatial dimensions, and a fundamental connection to hyperbolic conservation laws. We determine the evolution of a set of level set functions  $\{\phi_1(\mathbf{x},t), \phi_2(\mathbf{x},t), \phi_3(\mathbf{x},t)\}$  and the velocity field  $\mathbf{u}(\mathbf{x},t)$ . The location of a boundary  $\Gamma_i$  is defined by  $\phi_i(\mathbf{x},t)$  according to

$$\phi_i = \begin{cases} > 0 & \text{in } \Omega_i \\ 0 & \text{on } \Gamma_i \\ < 0 & \text{elsewhere} \end{cases} \quad (5)$$

and interface evolution is given by

$$\frac{\partial \phi_i}{\partial t} = -\mathbf{u} \cdot \nabla \phi_i. \quad (6)$$

Additionally, we require  $\phi_i$  to be a signed distance function, meaning that at any position  $\mathbf{x}$ ,  $|\phi_i(\mathbf{x})|$  is equal to the shortest distance from  $\mathbf{x}$  to  $\Gamma_i$ . Then  $\phi_i$  is a smooth function satisfying

$$|\nabla \phi_i| = 1. \quad (7)$$

For a single interface, defined by  $\phi(\mathbf{x},t)$ , the force  $\mathbf{F}$  in Eq. (3) can be written as

$$\mathbf{F} = [1/(\text{Re Ca})]\kappa(\phi)\nabla H(\phi), \quad (8)$$

where  $\kappa$  is the interface curvature (computed from  $\phi$ ) and  $H$  is the Heaviside function. The evolution of the velocity field and the interface is determined from the coupled solution of Eqs. (3), (4), and (6). For a two fluid system only a single level set function is needed and this description is complete. The treatment of a system of three or more fluids proceeds in a similar manner, where a unique level set function defines the boundary of each phase. This approach leads to problems at triple lines and other multiple junctions (i.e., quadruple points). A sketch of the methodology developed in Refs.[19]

and [28] is as follows: At a given point  $\mathbf{x}'$  in  $\Omega_i$  which is closer to  $\Gamma_{ij}$  than to  $\Gamma_{ik}$  it follows from the signed distance property that

$$\phi_i(\mathbf{x}') = -\phi_j(\mathbf{x}') > 0 > \phi_k(\mathbf{x}'). \quad (9)$$

If each element of  $\{\phi_1, \phi_2, \phi_3\}$  is evolved independently it is possible for this criterion to be violated. To avoid this we treat Eq. (9) as a constraint on  $\{\phi_1, \phi_2, \phi_3\}$ . Then it is possible to remove a degree of freedom by performing a linear projection of the level set functions onto a reduced set of variables, i.e.,  $\{\phi_1, \phi_2, \phi_3\} \mapsto \{\psi_A(\mathbf{x}, t), \psi_B(\mathbf{x}, t)\}$ . This is done as follows:

$$\psi_A = (2\phi_1 - \phi_2 - \phi_3)/\sqrt{6}, \quad (10)$$

$$\psi_B = (\phi_2 - \phi_3)/\sqrt{2}. \quad (11)$$

The inverse transformation  $\{\psi_A, \psi_B\} \mapsto \{\phi_1, \phi_2, \phi_3\}$  is

$$\theta_1 = 2\psi_A/\sqrt{6}, \quad (12)$$

$$\theta_2 = -\psi_A/\sqrt{6} + \psi_B/\sqrt{2}, \quad (13)$$

$$\theta_3 = -\psi_A/\sqrt{6} - \psi_B/\sqrt{2}, \quad (14)$$

$$\phi_1 = (\theta_1 - \theta_2 - \theta_3 + \min(\theta_1, \theta_2, \theta_3))/2, \quad (15)$$

$$\phi_2 = (-\theta_1 + \theta_2 - \theta_3 + \min(\theta_1, \theta_2, \theta_3))/2, \quad (16)$$

$$\phi_3 = (-\theta_1 - \theta_2 + \theta_3 + \min(\theta_1, \theta_2, \theta_3))/2. \quad (17)$$

By evolving  $\{\psi_A, \psi_B\}$  rather than  $\{\phi_1, \phi_2, \phi_3\}$  all of the interfaces remain well defined and mutually consistent at any multiple junction.

## V. NUMERICAL RESULTS

In order to determine which, if any, of the flows predicted in Fig. 4 occur we turn to numerical calculations. Steady state flow fields for several equilibrium conformations (labeled in Fig. 2) are determined. Symmetric conformations [(*sa*)  $\kappa_{321} = \kappa_{312} < 1$ ; (*sb*)  $\kappa_{321} = \kappa_{312} = 1$ ; (*sc*)  $\kappa_{321} = \kappa_{312} > 1$ ] as well as asymmetric conformations [(*da*)  $\kappa_{321} = 1, \kappa_{312} < 1$  and (*wa*)  $\kappa_{321} > 1, \kappa_{312} = 1$ ] are considered. In all cases the drop is placed between parallel plates moving at constant velocity with periodic boundaries in the horizontal direction. A box size of  $2 \times 1$  with  $a=1/8$  is used. Grid resolution is  $256 \times 128$ .

### A. Symmetric drops ( $\kappa_{312} = \kappa_{321}$ )

For the symmetric case in which  $\kappa_{312} = \kappa_{321} < 2$  the equilibrium configuration varies only in the extent to which the drop spreads across  $\Gamma_{12}$ . In the absence of any symmetry breaking instability only class A, B, and C flows can occur. For the equilibrium shapes *sa*, *sb*, and *sc*, as specified in Fig. 2, the computed steady state flow fields shown in Fig. 5 confirm this prediction. For a slender drop (*sa*, lowest  $\kappa_{312}$ ) we observe class A flow with no recirculation near *L* or *R*.

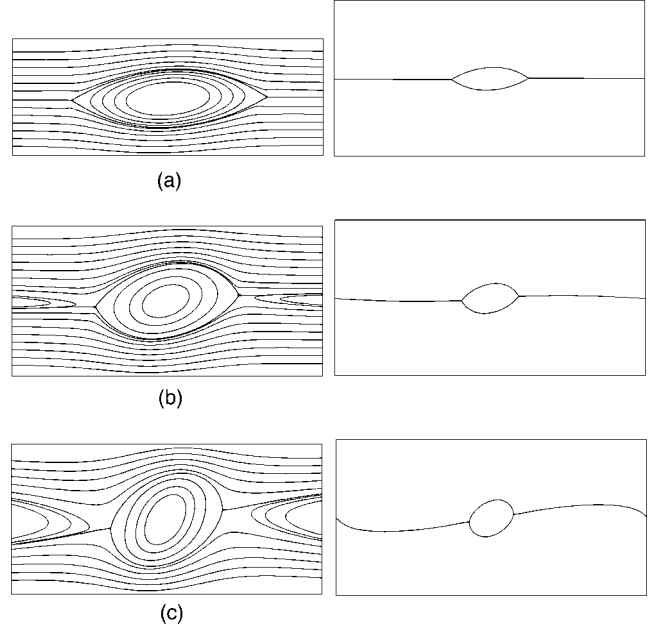


FIG. 5. Computed streamlines (near the drop) and interfacial shapes (over the entire system) for symmetric conformations: (a)  $\kappa_{321} = \kappa_{312} = 0.6, Ca = 0.125$  *sa* conformation. (b)  $\kappa_{321} = \kappa_{312} = 1, Ca = 0.075$ , *sb* conformation. (c)  $\kappa_{321} = \kappa_{312} = 4, Ca = 0.141$ , *sc* conformation.

However one cannot entirely eliminate the possibility of very narrow recirculating regions which are beyond the numerical resolution. At larger values of  $\kappa_{312}$  class B flow is observed with recirculating regions clearly present. Class C flow has not been observed for any value of  $\kappa_{312}$ . The *sb* and *sc* flows are qualitatively similar but the width of the recirculating region increases with  $\kappa_{312}$  as the drop becomes less elongated.

Shear also has a noticeable effect on the external interface and the triple lines. *L* and *R* lie below and above the centerline, respectively.  $\Gamma_{12}$  has an upward slope at *L* and *R* which is approximately equal to the slope of the line between *L* and *R*. Streamlines in the recirculating regions are nearly symmetrical, from which it can be deduced that the stable manifolds of *L* and *R* are similar in shape to the unstable manifolds (which lie on  $\Gamma_{12}$ ) and do not have high curvature. Unlike the simple drop scenario not only the drop shape is of interest but also the shape of  $\Gamma_{12}$  away from the drop. Since the system is periodic, the height of  $\Gamma_{12}$  at the box borders remains at a constant value. At a sufficient distance from the drop  $\Gamma_{12}$  has a downward slope. Because of this the box length is more relevant to the steady shape than in the case of a simple drop. In order to determine whether interface shapes near the drop are dependent on box size the results for different box lengths were compared. We found that the drop shape and the shape of  $\Gamma_{12}$  near the drop converged with increasing box length. Additionally the shape of the interfaces near the triple points is of interest and a few comments are pertinent here. In our numerical technique it is the balance of interfacial tension forces which drives the interfaces towards their equilibrium contact angles at a triple point. Interfacial tension is numerically resolved over a narrow re-

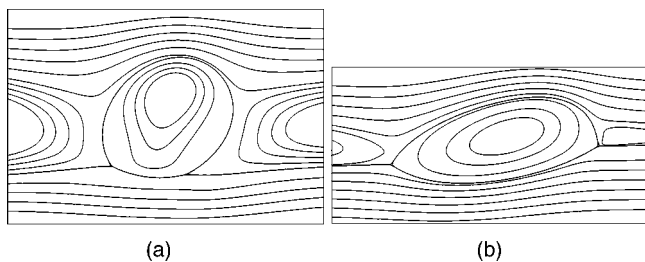


FIG. 6. Computed streamlines for asymmetric drops. (a)  $wa, \kappa_{312}=1, \kappa_{321}=1.8, Ca=0.019$ ; (b)  $da, \kappa_{312}=0.6, \kappa_{321}=1, Ca=0.33$ .

gion about the interface whose width is approximately one grid length on either side of the triple line. Thus the forces in the neighborhood of the triple point are resolved over a finite number of grid points. As grid resolution is increased, the area of this region decreases. We have done calculations at higher grid resolutions and found convergence in the shape of the interfaces and no change in the flow topology.

**B. Asymmetric drops ( $\kappa_{312} \neq \kappa_{321}$ )**

When  $\kappa_{312} \neq \kappa_{321}$  the flow is not symmetrical about the center line and class  $D$  flow may occur. Steady flows for two distinct asymmetric conformations ( $wa$  and  $da$  in Fig. 2) have been computed (Fig. 6). In both cases the center of mass of the drop lies above  $\Gamma_{12}$  and the drops “rolls” along  $\Gamma_{12}$ . While topologically equivalent, the two flows have significant differences. For the  $wa$  case  $\theta_1$  is acute and the recirculating regions are large while the streamlines are notice-

ably blunt near the drop. Significant curvature is evident in the manifolds in  $\Omega_1$ . Near the triple lines these manifolds appear to lie much closer to  $\Gamma_{13}$  than to  $\Gamma_{12}$ . For the  $da$  case  $\theta_1$  is obtuse and the recirculating regions are narrower and more similar to those observed for symmetric drops.

**VI. DISCUSSION AND CONCLUSIONS**

For a simple drop in shear flow at moderate viscosities there is a critical capillary number,  $Ca_{crit}$ , above which the drop has no steady shape and undergoes continuous deformation. In a three-dimensional system the drop can develop narrow necks, due to end pinching or the capillary instability, which undergo pinch-off, producing smaller drops. We refer to this as simple pinch-off. A broader range of instabilities is possible for interfacial drops which has yet to be addressed thoroughly. We conclude by discussing possible implications of the equilibrium conformation on the drop instability. The symmetric drop  $sb$  deforms at  $Ca_{crit}$  along the interface such that the distance between  $L$  and  $R$  increases with drop length [Fig. 7(a)]. In this case a three-dimensional drop could undergo pinch-off such that the subsequently formed drops remain on the external interface. This process, which we call interfacial pinch-off, differs from simple pinch-off because of the presence of the triple line. Simple pinch-off has been viewed as a singularity of the interface which occurs in finite time [29]. For small neck widths (close to the pinch-off event) the problem is locally axisymmetric and fluid is driven out of the neck due to interfacial tension induced pressure gradients. For interfacial pinch-off the triple lines eliminate the axisymmetry. Additionally the effect of line

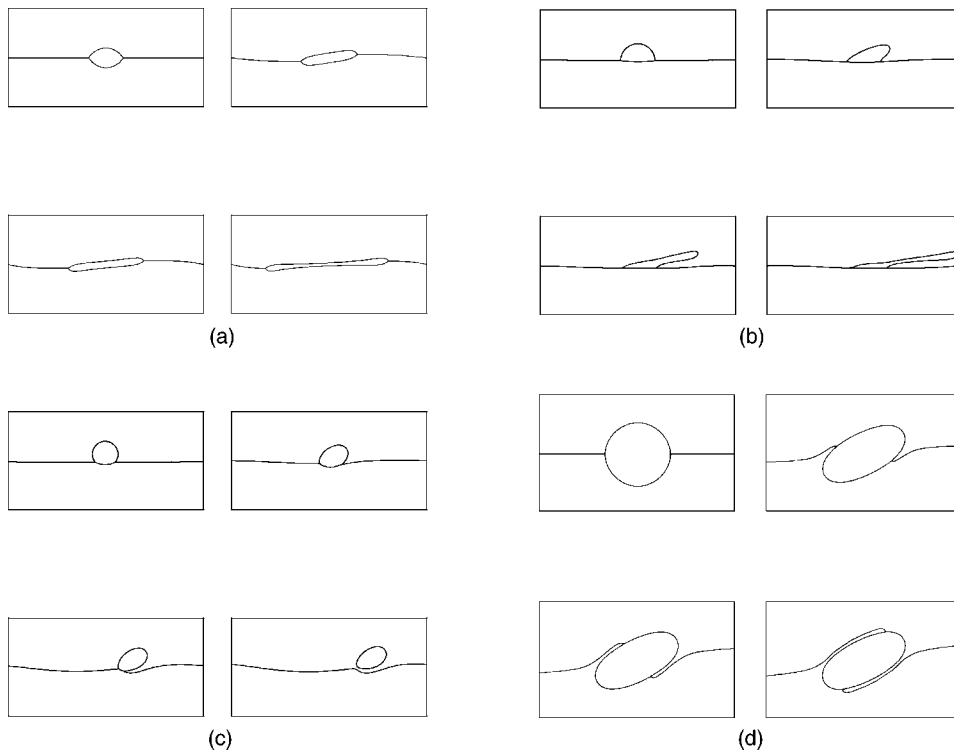


FIG. 7. Instabilities for several equilibrium conformations. (a)  $sb, \kappa_{312}=\kappa_{321}=1$ ; (b)  $da, \kappa_{312}=0.1, \kappa_{321}=1$ ; (c)  $wa, \kappa_{312}=1, \kappa_{321}=1.8$ ; (d)  $sc, \kappa_{312}=\kappa_{321}=10$ .

tension [30] could be significant. Any decrease in neck width would increase the curvature of the triple lines and thus would be opposed by positive line tension. Thus there is a competition between interfacial tension, which promotes breakup, and line tension, which stabilizes elongated drops. For the *da* conformation the drop also deforms [Fig. 7(b)] at  $Ca_{crit}$  but in this case it stretches into one of the external fluids such that  $L$  and  $R$  do not move apart. In this case simple pinch-off can occur away from  $\Gamma_{12}$ , producing a series of drops in the external fluid and a single drop remaining on the interface. Instabilities also exist for which the drop undergoes only finite deformation. For the *wa* conformation the drop does not “stick” to the external interface as much as it does for the *da* case (that is,  $\theta_1$  is smaller). Then the drop

may be removed completely from the external interface by the shear [Fig. 7(c)]. Finally, the change in topology described in Fig. 4 occurs because interfacial tension of the external interface resists drop rotation, which would increase the length of  $\Gamma_{12}$ . As  $\sigma_{12} \rightarrow 0$  (*sb*) this effect is lost and the drop resembles a simple drop where  $\Gamma_{12}$  is a passive material line. Then  $\Gamma_{12}$  may become unstable at low  $Ca$  where the drop is stable. In this case the flow resembles Fig. 3 and  $\Gamma_{12}$  wraps around the drop [Fig. 7(d)].

#### ACKNOWLEDGMENTS

This work was supported by IGERT-NSF Grant No. 9987577 and by NSF Grant No. DMR-0109610.

- 
- [1] M. Tjahjadi and J. M. Ottino, *J. Fluid Mech.* **232**, 191 (1991).  
 [2] R. G. Larson, *The Structure and Rheology of Complex Fluids* (Oxford University Press, New York, 1999).  
 [3] F. S. Bates, *Science* **251**, 898 (1991).  
 [4] S. Walheim, M. Ramstein, and U. Steiner, *Langmuir* **15**, 4828 (1999).  
 [5] C. Huang, M. O. de la Cruz, and B. W. Swift, *Macromolecules* **28**, 7996 (1995).  
 [6] L. Q. Chen, *Scr. Metall. Mater.* **29**, 683 (1993).  
 [7] A. J. Bray, *Philos. Trans. R. Soc. London, Ser. A* **361**, 781 (2003).  
 [8] I. Pagonabarraga, A. J. Wagner, and M. E. Cates, *J. Stat. Phys.* **107**, 39 (2002).  
 [9] M. E. Cates, V. M. Kendon, P. Bladon, and J. C. Desplat, *Faraday Discuss.* **112**, 1 (1999).  
 [10] F. J. Solis and M. O. de la Cruz, *Phys. Rev. Lett.* **84**, 3350 (2000).  
 [11] A. Onuki, *J. Phys.: Condens. Matter* **9**, 6119 (1997).  
 [12] T. Hashimoto, K. Matsuzaka, E. Moses, and A. Onuki, *Phys. Rev. Lett.* **74**, 126 (1995).  
 [13] A. Xu, G. Gonnella, and A. Lamura, *Phys. Rev. E* **67**, 056105 (2003).  
 [14] H. S. Jeon, Z. Shou, A. Chakrabarti, and E. K. Hobbie, *Phys. Rev. E* **65**, 041508 (2002).  
 [15] F. Corberi, G. Gonnella, and A. Lamura, *Phys. Rev. E* **62**, 8064 (2000).  
 [16] G. I. Taylor, *Proc. R. Soc. London, Ser. A* **146**, 501 (1934).  
 [17] J. M. Rallison, *Annu. Rev. Fluid Mech.* **16**, 45 (1984).  
 [18] H. A. Stone, *Annu. Rev. Fluid Mech.* **26**, 65 (1994).  
 [19] K. A. Smith, F. J. Solis, L. Tao, K. Thornton, and M. O. de la Cruz, *Phys. Rev. Lett.* **84**, 91 (2000).  
 [20] O. Kuksenok, D. Jasnow, J. Yeomans, and A. C. Balazs, *Phys. Rev. Lett.* **91**, 108303 (2003).  
 [21] A. Campos, K. Holland, and U. J. Wiese, *Phys. Lett. B* **443**, 338 (1998).  
 [22] H. A. Stone, A. Nadim, and S. H. Strogatz, *J. Fluid Mech.* **232**, 629 (1991).  
 [23] J. Guckenheimer and P. Holmes, *Nonlinear Oscillations, Dynamical Systems, and Bifurcations of Vector Fields* (Springer-Verlag, Berlin, 1983).  
 [24] E. B. Dussan-V, *Annu. Rev. Fluid Mech.* **11**, 371 (1979).  
 [25] M. Sussman, P. Smereka, and S. Osher, *J. Comput. Phys.* **114**, 146 (1994).  
 [26] Y. C. Chang, T. Y. Hou, B. Merriman, and S. Osher, *J. Comput. Phys.* **124**, 449 (1996).  
 [27] J. U. Brackbill, D. B. Kothe, and C. Zemach, *J. Comput. Phys.* **100**, 335 (1992).  
 [28] K. A. Smith, F. J. Solis, and D. L. Chopp, *Interfaces Free Boundaries* **4**, 263 (2002).  
 [29] J. Eggers, *Rev. Mod. Phys.* **69**, 865 (1997).  
 [30] P. Chen, J. Gaydos, and A. W. Neumann, *Langmuir* **12**, 5956 (1996).